Hyperfine Interactions 38 (1987) 471–498

INVERSE HOOK METHOD FOR MEASURING OSCILLATOR STRENGTHS FOR TRANSITIONS BETWEEN EXCITED ATOMIC STATES [1]

W.A. van WIJNGAARDEN, K.D. BONIN and W. HAPPER

Department of Physics, Princeton University, Princeton, N.J. 08544, U.S.A.

We describe an effective new method to measure the oscillator strengths for transitions between the excited states of atoms. The oscillator strength is determined by measuring changes in the angular distribution or polarization of fluorescence light emitted by atoms in the initial or final state of the transition of interest, after these atoms have been subject to the a.c. Stark shift of an off-resonant laser pulse. The physics of the situation is very similar to that of the conventional hook method with this difference: the roles of the atoms and the photons have been interchanged. We therefore call this new method *the inverse hook method*. The inverse hook method is relatively insensitive to the details of the atomic absorption lineshape and also to the temporal and spectral profile of the laser pulse. It yields absolute oscillator strengths and it is especially suitable for measurements of transitions between excited atomic states, including autoionizing states.

1. Introduction

Oscillator strengths or absolute atomic transition probabilities are needed for such different problems as the determination of the constituent concentrations of stellar matter [2] and the optimization of isotope separation by selective laser ionization [3–5]. There are several different definitions of oscillator strengths in the literature [6–8]. We shall use Corney's definition of an oscillator strength f_{ab} for a transition from an initial level a to a final level b [9],

$$f_{ab} = \frac{2m_e\omega_{ba}}{3\hbar e^2[J_a]} \sum_{m_b,m_a} |\langle am_a | \boldsymbol{D} | bm_b \rangle|^2 \tag{1.1}$$

where m_e is the electron mass, e is the electron charge, $\omega_{ba} = (E_b - E_a)/\hbar$ where E_a and E_b are the energies of levels a and b, $[J] = 2J + 1$ is the statistical weight of a level with electronic angular momentum J, m is the azimuthal quantum number and the electric dipole moment operator is $\boldsymbol{D} = e\sum_n \boldsymbol{r}_n$, where $\boldsymbol{r}_n$ is the position vector of the nth atomic electron. Note that the oscillator strength f_{ab} is positive if $E_a < E_b$, i.e. if an atom absorbs a photon to make a real transition from level a to level b. If $E_a > E_b$, i.e. if an atom emits a photon to make a real

transition from level a to level b, the oscillator strength f_{ab} is negative. Note that f_{ab} and f_{ba} are related by:

$$[J_b]f_{ba} = -[J_a]f_{ab}. \tag{1.2}$$

The oscillator strength is related to the Einstein spontaneous emission rate A_{ab} by the following expression.

$$A_{ab} = -\frac{2e^2\omega_{ab}^2}{m_e c^3} f_{ab}. \tag{1.3}$$

If the transition rates A_{ab} to all the lower lying levels b are known, the radiative lifetime τ_a of state a can be computed as follows.

$$\tau_a^{-1} = \sum_b A_{ab}. \tag{1.4}$$

The lifetime of a state alone is insufficient to determine the oscillator strengths for transitions from a level which has more than one decay channel.

A number of methods have been developed to measure oscillator strengths. These were recently discussed in an excellent review article by M. Huber and R. Sandeman [10]. The older methods, such as the hook [11] and absorption methods, measure the index of refraction or the absorption coefficient of an atomic vapor near the transition wavelength. These quantities are proportional to the product of the oscillator strength of the transition from level a to level b and $N_a/[J_a] - N_b/[J_b]$ where N_a and N_b are the atomic number densities in levels a and b respectively. The number density of the ground state can usually be approximated by the total atomic number density. Excited state densities however, particularly in electric discharges where the atoms are not in equilibrium, are more difficult to estimate. Hence, these methods are best suited to measured oscillator strengths for transitions originating from the ground state.

A number of methods [12–15] have been developed to take advantage of lasers. For example, the Autler-Townes method [13,14] uses a laser resonant with the transition of interest, to perturb the energy levels via an a.c. Stark interaction. For simplicity, we consider a two level atom whose states are at energies E_2 and E_1. In the absence of a laser, there will be a single fluorescence peak at frequency $\nu_0 = (E_2 - E_1)/h$. When a powerful laser of frequency ν_0 illuminates the atoms, sidepeaks at frequencies $\nu_0 \pm DE/h$ appear. Here D is the transition electric dipole moment and E is the laser electric field. The oscillator strength which by definition is a sum of squares of electric dipole matrix elements can then be found by measuring the spectral splitting. For a large spectral splitting, high electric fields are needed. These are available using either pulsed lasers or focussed CW lasers. In practice, pulsed lasers are not used since it is difficult to accurately determine the temporal profile of each laser pulse. A complication

arising from the use of focussed CW lasers is that the spatial profile is not uniform and different atoms interact with fields of various strengths. The fluorescent peaks are then smeared together yielding a broadened profile. Furthermore, there are usually several dipole moments D, corresponding to the different sublevels of the atom, so several sidepeaks are formed. The sidepeaks are also subject to Doppler and collisional broadening. Because of these problems, the Autler-Townes effect has not been widely used to measure oscillator strengths.

Our newly developed method, the inverse hook method [16], uses a pulsed laser to perturb a state via an a.c. Stark interaction. Unlike the Autler-Townes method it is relatively insensitive to both the temporal and spatial laser profiles. Although the method is closely analogous to the conventional hook method, it does not require knowledge of any atomic number density, and can therefore be readily used to measure oscillator strengths of transitions between excited states.

2. Overview of the inverse hook method

In this section we review the basic ideas and experimental procedures of an oscillator strength measurement by the inverse hook method. A more thorough discussion of the theory is presented in section 3, and experimental details of an actual measurement are presented in section 4. We shall refer to a simplified experimental sketch in fig. 1 and a heuristic theoretical sketch, fig. 2, in our discussion.

Two laser pulses of different frequencies are needed. The first or "exciting" pulse, EXC of fig. 1, propagates along the y axis and is linearly polarized along the z axis of a coordinate system. It is tuned to excite the atoms into an initial level, the populated level a of fig. 2. It is essential that the exciting pulse produce an anisotropic distribution of atoms among the sublevels of a. In the example of fig. 2, the excitation is caused by a two-photon transition, but a one-photon transition or any other excitation mechanism would be acceptable if the anisotropic excitation condition is met. Here we have assumed that level a has angular momentum $J_a \geq 1$ so that a linearly polarized excitation laser can create an anisotropic sublevel population distribution. If $J_a = 1/2$, one can use circularly polarized light to create different populations of the sublevels $|1/2\rangle$ and $|-1/2\rangle$. Finally, oscillator strengths for transitions between levels of angular momentum 0 and 1 can be determined by choosing the $J = 1$ level to be the populated level.

Shortly after the atoms are excited and before there has been appreciable spontaneous decay, a second pulse of laser light propagate through the atoms along the negative y axis. The frequency ω of the second or "light shift" laser is tuned close to but not equal to the resonant frequency $|\omega_{ab}|$ of the transition

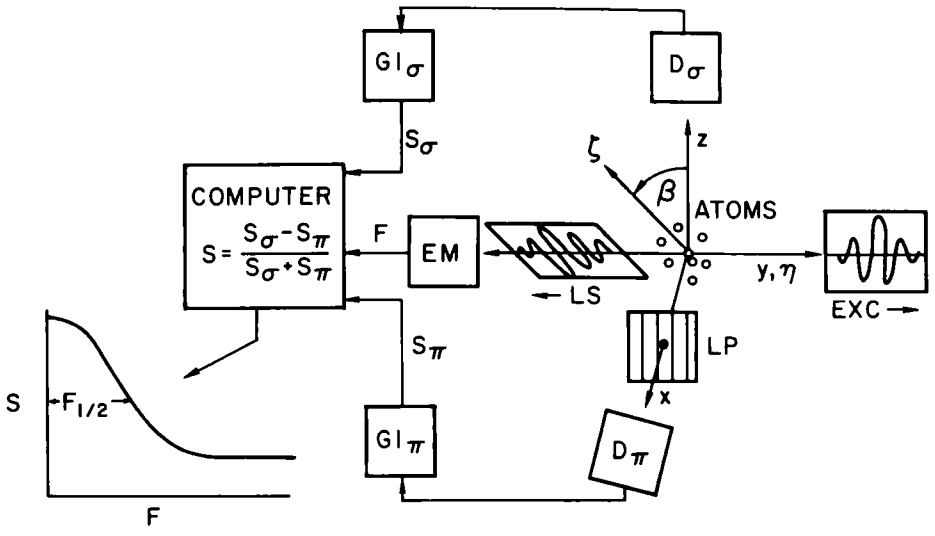

Fig. 1. Basic experimental arrangement. The laser pulses are shown just after they have passed through the atomic vapor. The atoms are first excited by laser pulse EXC. Later a "light shift" (LS) laser pulse from a second dye laser perturbs the atoms as is discussed in the text and is illustrated in fig. 2. An energy meter EM measures the energy of the LS pulse and sends this reading to a computer. Unpolarized and linear polarized fluorescence are detected by detectors D_σ and D_π. The fluorescent signals are input to gated integrators GI_σ and GI_π whose outputs S_σ and S_π are also transmitted to the computer. Finally, the computer analyzes the data an plots it as is shown in the figure.

from level a to level b for which the oscillator strength is to be measured. The light shift pulse is linearly polarized along a direction $\hat{\zeta}$ which is tilted by an angle $\beta = 54.74°$ from the z axis and which lies in the xz plane as shown in fig. 1. The beam of the light shift laser is intentionally speckled [17–19] with a random phase retardation plate (not shown), and the mean fluence $F(\text{ergs/cm}^2)$, averaged over many speckles is measured with the energy meter EM of fig. 1. One can use different optical path lengths to get the proper timing of the pulses, as is discussed in more detail in section 4.

The effect of the light shift pulse on the atoms is illustrated in fig. 2b. The light causes virtual transitions from sublevels of a to sublevels of b and back to different sublevels of a. After the light shift pulse, the distribution of population in the sublevels of a will have been modified as indicated in fig. 2c.

The changes in sublevel populations caused by the light shift laser are measured by observing changes in the fluorescence emitted by the excited atoms. The fluorescence corresponding to a particular decay branch is recorded by two detectors, D_σ and D_π of fig. 1, which record the σ and π fluorescence from the atoms. Not shown in fig. 1 are the optical filters or monochromators and lenses

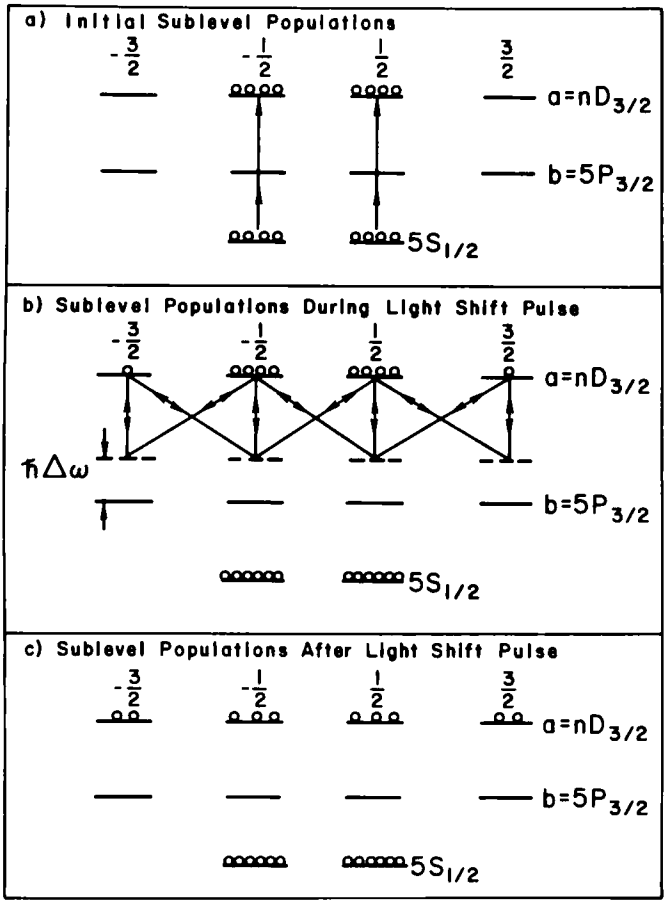

Fig. 2. Zeeman sublevel populations during experiment.

needed to isolate a given fluorescent wavelength and focus the fluorescence on the detectors. The detector D_σ, situated on the z axis records the total unpolarized fluorescence propagating along the z axis. The detector D_π is located on the x axis and detects fluorescence which has passed through a linear polarizer with its transmission axis parallel to the z direction. The signals from the two detectors are sent to two gated integrators GI, which are adjusted to begin integrating the photomultiplier signals after the light shift pulse has passed through the atomic sample. The gated integrators stop integrating after a few natural lifetimes of the excited atoms, and the two integrated outputs, S_σ and S_π, are transmitted to a small computer.

The electronic gains are adjusted to ensure that if fluorescence from unpolarized excited atoms were observed, one would find $S_\sigma = 2S_\pi$. Since truly unpolarized excited atoms are difficult to produce, a practical way to calibrate

the gains is now discussed. The atoms are excited with linearly polarized light whose polarization axis is tilted from the z axis by the "magic angle" 54.74°. Ordinary one-photon excitation or n-photon excitation can be used. The linear polarization ensures that only even multipole moments of atomic polarization are excited, up to a maximum multipolarity index of $L = 2n$ if $J_a \geq n$ where n is the number of photons absorbed in the transition. The magic tilt angle ensures that there is no longitudinal alignment ($L = 1$, $M = 0$), the only type of atomic polarization which can influence the signals S_π and S_σ in fig. 1. The electronic gains are then adjusted so that $S_\sigma = 2S_\pi$. No light shift laser should be used in the calibration step since the light shift pulse can upset the symmetry conditions needed for the calibration, but a magnetic field directed along the z axis is permissible.

The computer uses the calibrated signals to calculate a signal ratio

$$S(F) = \frac{S_\sigma - S_\pi}{S_\sigma + S_\pi} \tag{2.1}$$

and stores S along with the fluence F, which has also been transmitted to the computer from the energy meter EM. The denominator, $S_\sigma + S_\pi$, of the signal ratio is insensitive to the polarization and angular distribution of the fluorescence and is a measure of the total number of fluorescent photons emitted by the excited atoms. The numerator, $S_\sigma - S_\pi$, is sensitive to the alignment polarization of the excited atoms. Thus, the signal ratio S is a polarization-sensitive signal which is unaffected by shot-to-shot variations in the excitation efficiency of the atoms. The noise in the signal ratio is predominantly shot noise due to fluctuations in the number of photons detected by the photomultiplier tubes.

The measurement procedure described above is repeated many times for different fluences F to build up the signal ratio curve $S(F)$ indicated in fig. 1. An example of a real signal ratio curve is shown in fig. 3. The signal ratio of fig. 3 was obtained in a slightly different way than indicated in fig. 1 but the fluence halfwidth has the same physical significance, as we discuss in section 4. The signal ratio curve $S(F)$ has a fluence halfwidth $F_{1/2}$ which we define by

$$S(F_{1/2}) = \frac{S(0) + S(\infty)}{2}. \tag{2.2}$$

The curve $S(F)$ closely resembles a lorentzian depolarization curve on a fluence-independent background, i.e.

$$S(F) = \frac{1}{3}\left[1 - AB\varepsilon - \frac{AB(1-\varepsilon)}{1 + (F/F_{12})^2}\right]. \tag{2.3}$$

The parameters A, B and ε of (2.3) can be readily estimated as we shall show at the end of this section.

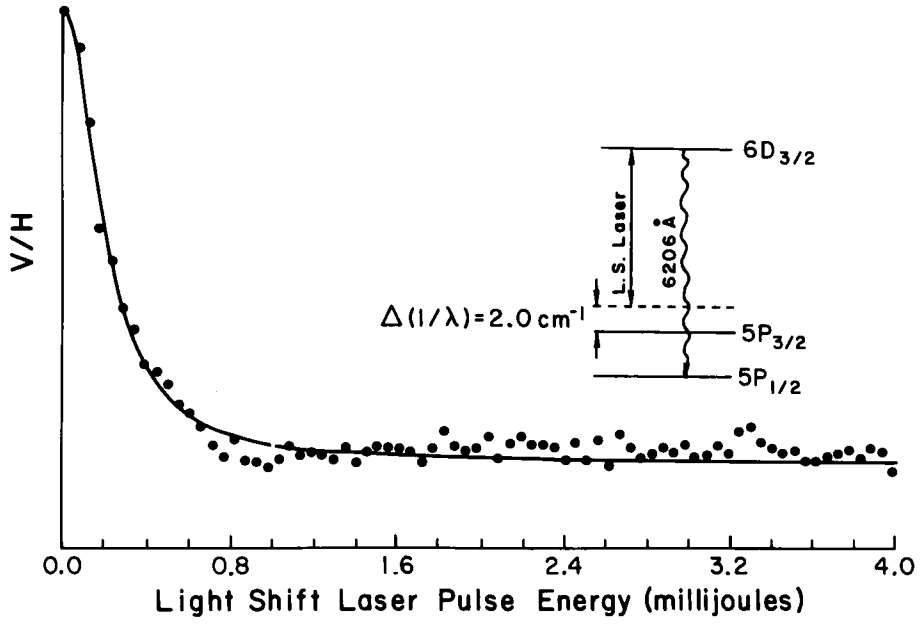

Fig. 3. A typical signal curve. The ratio of vertically polarized to horizontally polarized fluorescent fluence is plotted versus the light shift laser energy.

Only two quantities must be measured to determine oscillator strengths by the inverse book method:

1. the fluence halfwidth $F_{1/2}$
2. the light shift detuning $\omega - |\omega_{ab}|$.

Here ω is the frequency of the light shift laser and $|\omega_{ab}|$ is the resonant

Table 1
Halfwidth parameter $\theta_{1/2}$ and residual polarization parameter

J_a	ε	$\theta_{1/2}$	J_a	ε	$\theta_{1/2}$
1	0.3333	1.000	3/2	0	1.000
2	0.1429	1.031	5/2	0	1.260
3	0.0952	1.190	7/2	0	1.377
4	0.0722	1.297	9/2	0	1.444
5	0.0582	1.369	11/2	0	1.492
6	0.0490	1.423	13/2	0	1.526
7	0.0422	1.463	15/2	0	1.551
8	0.0372	1.493	17/2	0	1.573
9	0.0332	1.519	19/2	0	1.591
10	0.0300	1.539	21/2	0	1.603
–	0	1.753	∞	0	1.753

frequency of some transition of interest. From the fluence halfwidth $F_{1/2}$ we infer a characteristic fluence ΔF whose absolute value is given by

$$F_{1/2} = |\Delta F| \theta_{1/2}. \tag{2.4}$$

The dimensionless width parameter $\theta_{1/2}$, depends on the electronic angular momentum J_a of level a and is listed in table 1. The parameters $\theta_{1/2}$ of table 1 are the angles in radians needed to decrease the fluence dependent part of the signal ratio S by one half. These angles are all on the order of 1.5 radians or 90°.

We may determine the sign of ΔF from a formula which is derived in section 3

$$\frac{1}{\Delta F} = \frac{6\pi e^2}{m_e c\hbar} \sum_b \frac{\kappa_{ab} f_{ab}}{\omega_{ab}^2 - \omega^2} \tag{2.5}$$

where e is the electron charge, m_e is the electron mass, f_{ab} is the oscillator strength for a transition from level a to b and the coefficients κ_{ab} are

$$\kappa_{ab} = \begin{cases} \dfrac{2J_a - 1}{(J_a + 1)(2J_a + 3)} & \text{if } J_b = J_a + 1 \\ -\dfrac{2J_a - 1}{J_a(J_a + 1)} & \text{if } J_b = J_a \\ \dfrac{1}{J_a} & \text{if } J_b = J_a - 1 \end{cases} \tag{2.6}$$

According to (2.5) ΔF is an analytic function of the laser frequency ω with zeroes at the resonance frequencies $|\omega_{ab}|$, and with poles at certain other frequencies. It is not possible to take data exactly at the resonance frequencies $|\omega_{ab}|$ since many real transitions would be driven between levels a and b.

For laser frequencies ω in the immediate neighborhood of a resonant frequency $|\omega_{ab}|$, we may approximate (2.5) by (2.7)

$$f_{ab} \approx \frac{m_e c\hbar}{6\pi e^2} \frac{\omega_{ab}^2 - \omega^2}{\kappa_{ab} \Delta F} \tag{2.7}$$

to obtain an explicit formula for the oscillator strength f_{ab} in terms of the experimentally measureable quantities ΔF and $\omega - \omega_{ab}$. If transitions to several different levels b contribute to ΔF, a simultaneous determination of all of the corresponding oscillator strengths can be made by measuring the halfwidths $F_{1/2}$ as a function of the frequency ω of the light shift laser. One then uses (2.4) to construct a curve of ΔF versus ω, and fits this to the theoretical curve (2.5) with the oscillator strengths f_{ab} as free parameters. A real example of such a measurement and fit is shown in fig. 4.

An important consideration in any experiment is the signal to noise ratio. In

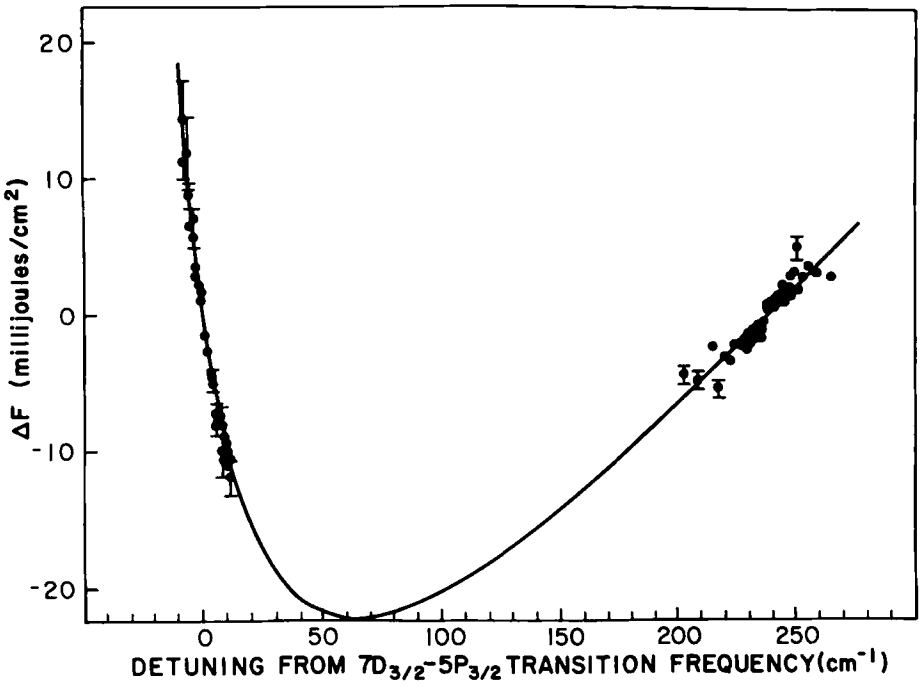

Fig. 4. A plot of ΔF versus light shift laser detuning.

the inverse hook method the noise for a carefully designed experiment can approach the shot noise limit where the noise is dominated by the statistical fluctuations in the number of fluorescent photons detected. The signal amplitude is determined by the parameters A, B and ε of formula (2.3). In this article we shall not derive formulae for these parameters which is done in ref. [1].

The parameter A measures the degree of initial alignment of the populated level a. One can imagine various ways to excite the atoms initially, eg. one photon or two-photon absorption, cascade, etc. An expression for A which is valid for all conditions of excitation is given by

$$A = \sqrt{\frac{20(2J_a-2)!}{(2J_a+3)!}} \sum_m \langle m \,|\, \rho_i \,|\, m \rangle \left[3m^2 - J_a(J_a+1)\right] \tag{2.8}$$

where $\langle m \,|\, \rho_i \,|\, m \rangle$ is the initial occupation probability of a sublevel of a with azimuthal quantum number m along the z axis.

The parameter ε is given by the following expression

$$\varepsilon = \tfrac{1}{3} C^2(J_a, J_a, 2; 1, 1) \tag{2.9}$$

Table 2
Branching factor $B(J_a, J_f)$

J_a	$J_f = J_a - 1$	$J_f = J_a$	$J_f = J_a + 1$
1	−4.899	2.450	−0.490
3/2	−4.000	3.200	−0.800
2	−3.742	3.742	−1.069
5/2	−3.666	4.190	−1.309
3	−3.666	4.583	−1.528
7/2	−3.703	4.938	−1.728
4	−3.761	5.265	−1.915
9/2	−3.830	5.571	−2.089
5	−3.906	5.858	−2.253
11/2	−3.985	6.131	−2.409
6	−4.068	6.392	−2.557
13/2	−4.151	6.642	−2.698
7	−4.235	6.882	−2.834
15/2	−4.319	7.113	−2.964
8	−4.402	7.337	−3.089
17/2	−4.485	7.554	−3.221
9	−4.568	7.765	−3.328
19/2	−4.649	7.970	−3.442
$\to \infty$	$-1.265\sqrt{J_a}$	$2.530\sqrt{J_a}$	$-1.265\sqrt{J_a}$

where we have used Rose's notation [20] in writing the Clebsch-Gordan coefficient C. It is a measure of how much atomic polarization is left after the atoms have been exposed to a speckled light shift laser pulse of very large fluence, and is hence called the residual polarization. Values of ε are listed in table 1.

The parameter B measures the sensitivity of the fluorescent polarization to the polarization of the excited atoms in level a. It is given by the following equation,

$$B = -2\sqrt{6}\,[J_a]\,W(1, 2, J_f, J_a; 1, J_a) \tag{2.10}$$

and is tabulated in table 2. B is proportional to a Racah coefficient W [20], which depends on the electronic angular momenta J_a of the populated level a and the electronic angular momentum J_f of the level f to which the atom makes a transition when it emits a fluorescent photon.

We should emphasize that the magnitudes of the parameters, A, B and ε have no direct bearing on oscillator strength measurements. They only determine the amplitude of the depolarization curve shown in fig. 3. Only the fluence halfwidth $F_{1/2}$ is needed to determine an oscillator strength. By choosing different fluorescent decay channels for observation, one can obtain depolarization curves of opposite signs, corresponding to the opposite signs of B in table 2, but the halfwidths $F_{1/2}$ of the curves for the two fluorescent channels will be the same.

Thus, one can choose the fluorescent decay channel for experimental convenience, for example, to minimize instrumental scatter from the lasers or to maximize the magnitude of B.

3. Theory

We begin by considering the response of an excited atom to the electric field of the light shift laser, which we write as

$$\boldsymbol{E} = \boldsymbol{\mathscr{E}}\, e^{-i\omega t} + \boldsymbol{\mathscr{E}}^*\, e^{i\omega t}. \tag{3.1}$$

The field amplitude $\boldsymbol{\mathscr{E}}$ is a function of time which varies slowly with respect to the laser frequency ω. For example, $\boldsymbol{\mathscr{E}}$ will typically be a pulse envelope which rises and falls in a few nanoseconds. The interaction of the electric dipole moment $\boldsymbol{D}$ of the atom and the electric field of the light is

$$V = -\boldsymbol{D}\cdot\boldsymbol{E}. \tag{3.2}$$

We shall consider excited atoms in an initially populated level a like that of fig. 2. We suppose that the level has electronic angular momentum J_a and that the hyperfine structure can be ignored. As we mentioned in connection with our earlier discussion of fig. 2b, the frequency of the light shift laser is sufficiently detuned from resonance that it can only transfer atoms between the sublevels $|m\rangle$ of level a. We assume that these sublevels are quantized along the z axis of fig. 1 and the azimuthal quantum number m is defined by

$$J_z|m\rangle = m|m\rangle \tag{3.3}$$

where J_z is the projection of the electronic angular momentum operator along the z direction. We denote the probability amplitudes of the sublevels $|m\rangle$ by $c(m)$. The coupling of these amplitudes by the light shift laser (i.e. by the virtual transitions sketched in fig. 2b) is described by the interaction-picture differential equation

$$i\hbar\dot{c}(m) = \sum_{m'} \langle am|H|am'\rangle c(m'). \tag{3.4}$$

We assume that the light shift pulse is of such short duration that coupling terms due to hyperfine structure, magnetic fields etc. can be neglected. The matrix elements $\langle m|H|m'\rangle$ of (3.4) are given by second order perturbation theory applied to the interaction (3.2), i.e.

$$\langle m|H|m'\rangle = -\sum_{\mu b} \frac{\langle am|\boldsymbol{\mathscr{E}}\cdot\boldsymbol{D}|b\mu\rangle\langle b\mu|\boldsymbol{\mathscr{E}}^*\cdot\boldsymbol{D}|am'\rangle}{\hbar(\omega_{ba}+\omega)} - \sum_{\mu b} \frac{\langle am|\boldsymbol{\mathscr{E}}^*\cdot\boldsymbol{D}|b\mu\rangle\langle b\mu|\boldsymbol{\mathscr{E}}\cdot\boldsymbol{D}|am'\rangle}{\hbar(\omega_{ba}-\omega)}. \tag{3.5}$$

The denominators contain the Bohr frequencies

$$\omega_{ba} = \frac{E_b - E_a}{\hbar} \tag{3.6}$$

for transitions between level b with energy E_b and level a with energy E_a.

The interaction (3.2) has odd parity and therefore cannot couple $|m\rangle$ and $|m'\rangle$ in first order or in any odd order of perturbation theory. The perturbation expansion parameter for conditions of interest in these experiments is

$$\left(\frac{\omega_r}{\Delta\omega}\right)^2 \approx \frac{1}{\Delta\omega T} \leq 10^{-3} \tag{3.7}$$

where $\omega_r \approx \mathscr{E} D_{ab}$ is the Rabi frequency, $\Delta\omega = \omega - |\omega_{ab}|$ is the detuning frequency, and T is the duration of the light shift pulse. We have assumed $(\omega_r^2 T/\Delta\omega) \approx 1$ which corresponds to a phase angle of about one radian. The small numerical value of 10^{-3} is obtained for representative parameters $T \approx 5$ nsec and $\Delta\omega = 2\pi c \times 1\ \mathrm{cm}^{-1}$. Thus, (3.7) implies that no higher order coupling terms are needed in addition to the second-order terms of (3.5).

The first term on the right of (3.5) describes a virtual transition from sublevel $|am'\rangle$ to sublevel $|b\mu\rangle$ with the creation by $\mathscr{E}^*$ of a photon of energy $\hbar\omega$, followed by a transition from $|b\mu\rangle$ to $|am\rangle$ with reabsorption of the photon. The second term on the right of (3.5) describes a similar process in which a photon is first absorbed and then recreated. Since we assume that $\omega \approx |\omega_{ba}|$, one of the energy denominators of (3.5) will be very small compared to the other, and the term associated with the small energy denominator will make almost all of the contribution to $\langle m|H|m'\rangle$. This dominant term corresponds to creation and destruction of photons in an order which nearly converses energy for the virtual transitions.

We shall consider the special case of laser light which is linearly polarized along the ζ axis of the "tilted" coordinate system $\xi\eta\zeta$ of fig. 1. The electric field amplitudes of (3.1) can be written as

$$\mathscr{E} = \mathscr{E}\hat{\zeta} \tag{3.8}$$

where $\hat{\zeta}$ is a unit vector along the ζ axis. The Hamiltonian matrix $\langle m|H|m'\rangle$ of (3.5) can be diagonalized if we choose basis states $|m\}$ for level a which are quantized along the direction $\hat{\zeta}$, i.e.

$$J_\zeta |m\} = m|m\} \tag{3.9}$$

where $J_\zeta = \hat{\zeta}\cdot\boldsymbol{J}$. We shall use curly kets $|m\}$ to distinguish sublevels quantized along $\hat{\zeta}$ from sublevels $|m\rangle$ quantized along $\hat{z}$.

The Hamiltonian (3.5) can now be written as

$$H = -\mathscr{E}^2 \sum_m \alpha(m)\,|am\}\{am|, \tag{3.10}$$

The polarizability $\alpha(m)$ of the state $|m\}$ can be calculated from (3.5) by means of the Wigner-Eckart theorem and the definition (1.1) of the oscillator strength to be

$$\alpha(m) = \sum_b \frac{3e^2 f_{ab}}{m_e(\omega_{ab}^2 - \omega^2)} C^2(J_b, 1, J_a; m, 0). \tag{3.11}$$

The relevant Clebsch-Gordan coefficients are

$$C^2(J_a+1, 1, J_a; m, 0) = \frac{(J_a+1)^2 - m^2}{(J_a+1)(2J_a+3)}$$

$$C^2(J_a, 1, J_a; m, 0) = \frac{m^2}{J_a(J_a+1)}$$

$$C^2(J_a-1, 1, J_a; m, 0) = \frac{J_a^2 - m^2}{J_a(2J_a-1)}. \tag{3.12}$$

The time evolution operator is

$$U = \exp\left\{\frac{-i}{\hbar}\int_{t_i}^{t_f} H\,dt\right\} = \sum_m e^{-i\phi(m)} |m\}\{m|. \tag{3.14}$$

The phases follow from (3.10) and are

$$\phi(m) = -\frac{2\pi\alpha(m)}{c\hbar} F. \tag{3.15}$$

The fluence F is related to the laser intensity I

$$I = c\mathscr{E}^2/2\pi \tag{3.16}$$

by

$$F = \int_{t_i}^{t_f} I\,dt. \tag{3.17}$$

For future reference we note that the phases can be written as

$$\phi(m) = \frac{m^2 F}{(2J_a-1)\Delta F} + \phi_0 \tag{3.18}$$

where ϕ_0 is independent of m. The parameter ΔF is given by

$$\frac{1}{\Delta F} = \frac{6\pi e^2}{m_e c\hbar} \sum_b \frac{\kappa_{ab} f_{ab}}{\omega_{ab}^2 - \omega^2} \tag{3.19}$$

The coefficients κ_{ab} follow from (3.12) and are

$$\kappa_{ab} = \begin{cases} \dfrac{2J_a - 1}{(J_a + 1)(2J_a + 3)} & \text{if } J_b = J_a + 1 \\ -\dfrac{2J_a - 1}{J_a(J_a + 1)} & \text{if } J_b = J_a \\ \dfrac{1}{J_a} & \text{if } J_b = J_a - 1. \end{cases} \tag{3.20}$$

There is an interesting physical meaning to (3.14) which will help to clarify the significance of the inverse hook method. According to the correspondence principle of quantum mechanics, atoms in a superposition of the adjacent azimuthal quantum states $|m\}$ and $|m-1\}$ will rotate about the ζ axis at a rate

$$\omega_m = \frac{\mathrm{d}}{\mathrm{d}t}[\phi(m) - \phi(m-1)] = \frac{2m-1}{2J_a - 1}\frac{I}{\Delta F}. \tag{3.21}$$

The total rotation angle of the atoms is

$$\int \omega_m \, \mathrm{d}t = \frac{2m-1}{2J_a - 1}\theta \tag{3.22}$$

where the characteristic twist angle is

$$\theta = F/\Delta F. \tag{3.23}$$

From (3.22) and (3.23) we see that $|\Delta F|$ is the laser pulse fluence needed to rotate atoms with their spins "pointing north" (i.e. atoms with $m = J_a$) by one radian. The sign of the rotation angle is the same as the sign of ΔF. Atoms with their spins pointing south (i.e. atoms with $m = -J_a + 1$) will rotate by one radian in the opposite direction. The linearly polarized light shift laser *twists* the atomic spin distribution uniformly about the polarization of the light. We may therefore call the unitary operator U of (3.14) a *torsion operator*.

We denote the initial density matrix which described the atoms in level a before the light shift pulse by ρ_i. After the light shift pulse has caused the changes indicated in fig. 2, the atoms in state a will be described by the final density matrix ρ_f given by

$$\rho_f = U\rho_i U^\dagger \tag{3.24}$$

where U was given by (3.14). We shall assume that before the light shift pulse, the atoms have pure alignment polarization, i.e. the populations of the sublevels $|m\rangle$ are given by

$$\langle m|\rho_i|m\rangle = C' + D'm^2 \tag{3.25}$$

where C' and D' are constants. We also assume that ρ_i has no off-diagonal matrix elements between the basis states $|m\rangle$. Purely aligned atoms are produced when linearly polarized light is used to excite atoms from an unpolarized ground state.

The population changes caused by the light shift laser (see fig. 2) can be detected by observing the resulting changes in the polarization or angular distribution of fluorescent light, as indicated in fig. 1. The power P of fluorescent light reaching the detector is given by [21]

$$P = N\, e^{-t/\tau_a}\, \mathrm{Tr}\left[\mathscr{L}\rho_f\right] \tag{3.26}$$

where τ_a is the natural lifetime of the fluorescing atoms in level a, and N is an overall constant which accounts for the number of excited atoms, the solid angle subtended by the detector, and the transmission efficiency of the filters and polarizers etc. The fluorescent light operator $\mathscr{L}$ describes how much fluorescent light will reach the detector through the polarization analyzing devices placed between the fluorescing atoms and the detector. For the case of a polarization analyzer which passes light linearly polarized along the unit vector $\hat{u}$, we can write

$$\mathscr{L} = B_0 + B_2 \sum_M Y_{2M}(\hat{u}) T^{\dagger}_{2M}. \tag{3.27}$$

As was shown in ref. [21], the coefficients B_0 and B_2 depend on the electronic angular momentum J_a of the excited atom and the angular momentum J_f of the level in which the atom is left after emission of a fluorescent photon. $Y_{2M}(\hat{u})$ is the value of the spherical harmonic at the location $\hat{u}$ on the unit sphere and the tensor T_{2M} is defined in the usual way as follows [21]:

$$T_{LM} = \sum_m |Jm\rangle\langle Jm - M|(-1)^{m-M-J} C(J, J, L; m, M-m). \tag{3.28}$$

For inverse hook measurements, we integrate the fluorescent power for several natural lifetimes as indicated in fig. 1. It is shown in ref. [1] that the integrated fluorescence power or fluorescent fluence is given by

$$S(\hat{u}) = 1 + \frac{AB}{2}\sqrt{\frac{4\pi}{5}}\, Y_{20}(\hat{u}) V(\theta, \beta) \tag{3.29}$$

where

$$V(\theta, \beta) = \sum_M d^2_{0M}(\beta) v^{22}_M(\theta) d^2_{M0}(-\beta) \tag{3.30}$$

and

$$v^{22}_M(\theta) = \sum_q C^2\left(J_a, J_a, 2; \frac{M}{2} + q, \frac{M}{2} - q\right) \cos\frac{qM\theta}{J_a - 1/2}. \tag{3.31}$$

Here A, given by (2.8), is a measure of the degree of initial alignment of the populated level a and B, given by (2.10), determines the sensitivity of the fluorescent polarization to the polarization of the excited atoms in level a. The summation index q is either an integer or a half-integer depending on M and on whether J_a is an integer or a half-integer. $d^2_{0M}(\beta)$ is a Wigner function for the special case of a rotation by an angle β around the y of η axis. In ref. [1] it was shown that $V(\theta, \beta)$ is maximized when $\beta = \beta_{\text{opt}}$ where

$$\sin^2\beta_{\text{opt}} = \frac{2}{3(1+\varepsilon)} \tag{3.32}$$

and ε was given by (2.9). For half-integer J_a where $\varepsilon = 0$, it follows from (3.32) that $\beta_{\text{opt}} = 54.74°$, the magic angle. For integer values of J_a, β_{opt} is somewhat less than 54.74° because ε is a small positive number. For example, if $J_a = 1$, we find $\varepsilon = 1/3$ and $\beta_{\text{opt}} = 45°$.

The signal given by (3.29) would be generated if a light shift laser with spatially uniform fluence were used in an experiment. Since this signal is a superposition of functions periodic in the laser fluence, it also will depend periodically on the laser fluence. In practice pulsed dye lasers usually have poor transverse mode structure and are spatially nonuniform. A much more practical experimental procedure which leads to good results, is to use a light shift laser for which the spatial distribution of fluence is as inhomogeneous as possible, i.e. a laser with a fully developed speckle distribution. Some of the experimental advantages of a speckled laser will be discussed in the next section.

If the mean fluence of a laser, averaged over many speckles is F, then the probability of finding a local fluence between F' and $F' + \mathrm{d}F'$ is [18]

$$P(F')\,\mathrm{d}F' = \frac{\mathrm{e}^{-F'/F}}{F}\mathrm{d}F'. \tag{3.33}$$

There will be a distribution of twist angles θ experienced by the excited atoms, with atoms in a bright speckle experiencing large twists and atoms in dim speckles experiencing small twists. We may account for the speckled laser beam by replacing $v^{22}_M(\theta)$ with a mean value $\bar{v}^{22}_M(\theta)$ averaged over the distribution (3.33).

$$\bar{v}^{22}_M(\theta) = \sum_q C^2\left(J_a, J_a, 2; \frac{M}{2}+q, \frac{M}{2}-q\right)\frac{1}{1+\left(\dfrac{qM\theta}{J_a - 1/2}\right)^2}. \tag{3.34}$$

Substituting the well known algebraic expressions for the Wigner functions into (3.30) we find that

$$\bar{V}(\theta, \beta) = \frac{(3\cos^2\beta - 1)^2}{4} + \tfrac{3}{4}\sin^2 2\beta \bar{v}^{22}_1(\theta) + \tfrac{3}{4}\sin^4\beta \bar{v}^{22}_2(\theta). \tag{3.35}$$

The theoretical halfwidths $\theta_{1/2}$ of the curves are given by

$$\bar{V}(\theta_{1,2}, \beta) = \frac{\bar{V}(0, \beta) + \bar{V}(\infty, \beta)}{2}. \tag{3.36}$$

Equation (3.36) can be solved numerically to find $\theta_{1/2}(\beta)$. From (3.30) and (3.31) we infer that $\bar{V}$ is an even function of θ so (3.36) has two solutions $\theta_{1/2}(\beta)$ where we arbitrarily set $\theta_{1/2}(\beta) > 0$. The width parameters $\theta_{1/2}$ for $\beta = 54.74°$ are listed in table 1 for $J_a \leq 10$. According to (3.23) the experimental halfwidth parameter $F_{1/2}$ is related to $\theta_{1/2}$ by

$$F_{1/2} = \theta_{1/2} |\Delta F|. \tag{3.37}$$

This equation is extremely important since it provides a relation between an experimentally measurable quantity $F_{1/2}$ and a theoretically significant parameter ΔF from which oscillator strengths can be easily inferred with the aid of (3.19). $F_{1/2}$ will always be a positive quantity since it is the fluence which causes the inverse hook signal to drop from its initial value halfway to its final value as illustrated in fig. 1. It is found by fitting the experimental data to the signal curve $\bar{V}(\theta, \beta)$ given by (3.35). For data with the usual experimental error, one can approximate $\bar{V}$, a weighted sum of Lorentzian curves of different halfwidths, by a single Lorentzian curve, i.e. we set

$$\bar{V}(\theta, 54.74°) \approx \frac{1 - \varepsilon}{1 + (\theta/\theta_{1/2})^2} + \varepsilon. \tag{3.38}$$

In this way one can conveniently determine the fluence halfwidth to an accuracy of a few percent.

4. Experimental discussion

The inverse hook method was used to determine oscillator strengths for the $nD_{3/2} \rightarrow 5P_{3/2,1/2}$ ($n = 6, 7$) transitions in rubidium. Rubidium, an alkali element, was chosen since it can be simply modelled as consisting of an outer electron interacting with a central potential generated by the nucleus and closed inner electron shells. Oscillator strengths can then be estimated in a fairly reliable way using the Coulomb approximation of Bates and Damgaard [22], and compared with values obtained experimentally. The $nD_{3/2} \rightarrow 5P_{3/2,1/2}$ ($n = 6, 7$) transitions were selected since their transition wavelengths lie in the visible region of the spectrum where dye lasers operate readily. In addition, the $6D_{3/2}$ (or $7D_{3/2}$) level can be populated by a two-photon excitation from the $5S_{1/2}$ ground state using 6969 Å (or 6605 Å) laser light.

The rubidium metal (^{85}Rb) was contained in an evacuated cylindrical pyrex glass cell, 8 inches in length and 1 inch in diameter. The cell was located in an oven heated by jets of hot air. Typically, data was taken at a temperature of 120 °C corresponding to a rubidium number density of about 2×10^{13} cm^{-3} [23]. At lower temperatures, the fluorescent signals were smaller and the shot noise was increased. The light shift signal widths, which will be discussed shortly, exhibited no dependence on cell temperatures between 80 °C and 120 °C corresponding to number densities of 10^{12} and 2×10^{13} cm^{-3}. This was not surprising since the parameters the inverse hook method uses to determine oscillator strengths, namely the fluence halfwidth and the laser detuning are expected to be independent of the number density. At very high number densities radiation trapping, parasitic lasing and collisions may be expected to degrade the signal to noise ratio.

The excitation and light shift dye lasers were pumped by a frequency doubled Nd : YAG laser at a 20 Hz repetition rate as is shown in fig. 5. The 4 nsec light shift pulse was delayed with respect to the excitation pulse by about 15 nsec due to its longer path to the cell containing the rubidium vapor. The excitation laser is linearly polarized along the z axis. It excites the $|\pm 1/2\rangle$ sublevels of the $n\mathrm{D}_{3/2}$ level equally if the ground state $5\mathrm{S}_{1/2}$ is unpolarized. A single hyperfine level could not be excited since the laser linewidth of about 0.05 cm^{-1} or 1.5 GHz was much greater than the hyperfine splitting of either the $6\mathrm{D}_{3/2}$ or $7\mathrm{D}_{3/2}$ level. For the $6\mathrm{D}_{3/2}$ state of ^{85}Rb, the magnetic dipole constant $a = 2.32$ MHz and the electric quadrupole hyperfine constant $b = 1.62$ MHz [24].

To determine how the light shift laser perturbed the atoms, the fluorescence polarization was monitored. It was desirable to integrate the fluorescent intensity over an interval encompassing several natural lifetimes of the populated state to minimize the effect of shot noise. The observed lifetime of the $6\mathrm{D}_{3/2}$ and $7\mathrm{D}_{3/2}$ levels was about 250 nsec. Unfortunately, a substantial amount of electric polarization was transferred to the nucleus via the hyperfine interaction during the several hundred nanosecond integration time [24].

For most atoms the loss of electronic polarization to the nucleus is not a problem since the hyperfine interaction is either very large, facilitating excitation of a single hyperfine level, or the hyperfine interaction is too small to noticeably degrade the electronic polarization. For atoms whose nuclei have zero spin, as is the case for half of the nuclei in the Periodic Table, there is no hyperfine interaction. ^{85}Rb is an example of the difficult intermediate case where the hyperfine interaction is neither negligible nor large enough for a single hyperfine level to be excited.

To prevent the transfer of electronic polarization to the nucleus, the nuclear spin was partially decoupled from the electron angular momentum by a magnetic field directed along the z axis. A 14 gauss field was generated by a pair of

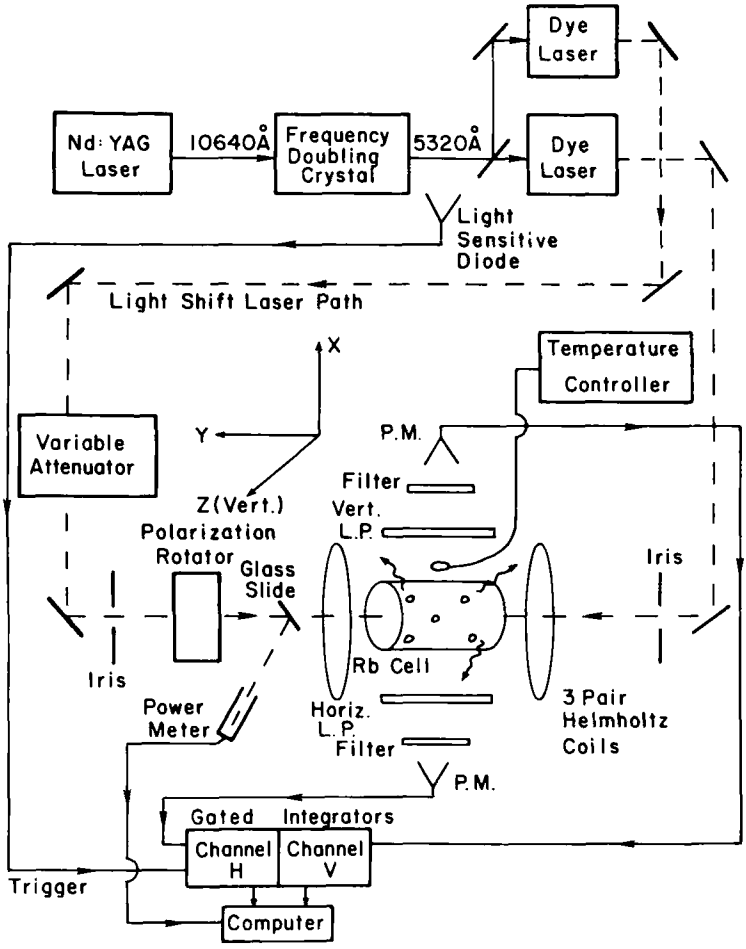

Fig. 5. Schematic diagram of the apparatus used to measure oscillator strengths with the inverse hook method.

Helmholtz coils. The magnetic field causes the electron angular momentum to precess during the light shift pulse. We have shown [1] that such a low field broadens the signal halfwidths by less than 2%. Since this 2% effect was much less than the total 20% uncertainty estimated for our measurements, the final oscillator strengths were not corrected for the effect of the magnetic field.

We shall now discuss the actual apparatus and procedure employed to determine the oscillator strengths using the inverse hook method. The light shift laser was nearly resonant with the $nD_{3/2} \rightarrow 5P_{3/2}$ or the $nD_{3/2} \rightarrow 5P_{1/2}$ ($n = 6, 7$) transition. The light beam output from the light shift dye laser was polarized

along the vertical direction. The polarization axis was subsequently rotated through an angle $\beta = 54.74°$ in order to maximize the light shift signal as shown in fig. 5. Part of the pulse was reflected into an energy meter by a glass side. Using the reflection coefficients of the glass slide, as well as those of the front and back cell windows, the amount of laser energy E perturbing the rubidium in the cell was determined. The excitation and light shift laser beams were aligned to pass through two irises located on either side of the cell. Dividing the laser energy E by the iris area ($A = 0.20$ cm^2), the light shift fluence $F = E/A$ was obtained.

Fluorescent light was detected along the $\pm x$ axis as shown in fig. 5. In each channel, detected light passed through a linear polarizer and was then directed through an interference filter before finally being focussed onto a photomultiplier. The detected fluorescence resulted from the transition of the $n\mathrm{D}_{3/2}$ populated level to one of the 5P levels. The interference filter transmitted the wavelength corresponding to the transition having the greater detuning from the light shift laser frequency so as to minimize detected laser scatter. The photomultiplier signals were electronically integrated for about 500 nsec. The integration starting time which began about 10 nsec after the end of the light shift pulse, together with the narrow bandwidth (20 Å) of the interference filter, reduced detected laser scatter to a negligible amount. Finally, the integrator signals and the light shift pulse energy were sent to an Apple IIe computer for analysis.

In our experiments, small detunings of typically a few cm^{-1} were used. The light shift laser detuning was fixed by pressurizing the laser oscillator with up to 18 psi of freon (CF_2Cl_2, commercially called Freon 12). To determine the relationship between the freon pressure and the detuning, freon was leaked out of the cavity. The change in laser wavelength was monitored by counting interference fringes produced by an etalon, while simultaneously determining the rubidium resonance frequency from the optogalvanic signal of a rubidium discharge lamp [25]. The detuning was determined to within a fraction of a free spectral range, which for an etalon cavity of length $L = 3.94$ cm is $(1/2\mathrm{L}) = 0.127$ cm^{-1}.

The effect of the light shift laser was studied by measuring the vertical fluorescent fluence given by (3.29),

$$S(\hat{z}) = 1 + \frac{AB}{2}\overline{V} \tag{4.1}$$

and the horizontal fluorescent fluence given by (3.29)

$$S(\hat{y}) = 1 - \frac{AB}{4}\overline{V}. \tag{4.2}$$

Using (3.35) to evaluate $\overline{V}$ at the magic angle $\beta = 54.74°$, the fluorescent fluences (4.1) and (4.2) become the following.

$$S(\hat{z}) = 1 + \frac{AB}{2} \frac{1}{1 + (F/\Delta F)^2} \tag{4.3}$$

$$S(\hat{y}) = 1 - \frac{AB}{4} \frac{1}{1 + (F/\Delta F)^2}. \tag{4.4}$$

In our experiment a ratio of $S(\hat{z})$ to $S(\hat{y})$ was determined to normalize to the shot-to-shot pulse energy fluctuation of the excitation laser. the fluorescent fluence ratio

$$R = \frac{S(\hat{z})}{S(\hat{y})} \tag{4.5}$$

found using (4.3) and (4.4) is given by the following.

$$R = \frac{1 + \frac{AB}{2} \frac{1}{1 + (F/\Delta F)^2}}{1 - \frac{AB}{4} \frac{1}{1 + (F/\Delta F)^2}}. \tag{4.6}$$

This may be simplified since the magnitude of the parameter A which describes the initial sublevel population anisotropy of level a is small relative to the constant background. The fluorescent fluence ratio can then be approximated as follows.

$$R = 1 + \frac{3}{4} AB \frac{1}{1 + (F/\Delta F)^2} \tag{4.7}$$

Note that if the two detector sensitivities are different, the fluence-dependent term of (4.7) remains proportional to a Lorentzian curve with halfwidth ΔF. Hence, unlike the case shown in fig. 1 where σ and π light are detected, the relative detector calibration is not necessary.

For each run, taken at a fixed detuning, data from nearly 4000 laser shots were accumulated. During a run, the light shift pulse energy was varied using an adjustable attenuator. The ratio of the $S(\hat{z})$ and $S(\hat{y})$ signals resulting from each laser shot was computed. Next the fluence axis was divided into typically 50 intervals. The average value of the raw data ratios lying in each fluence interval was computed and plotted.

The fluence halfwidth corresponding to a detuning $\omega - |\omega_{ab}|$, was found using a least squares fitting routine to select the Lorentzian curve best matching the data. Sample data runs taken at fixed detunings are shown in fig. 6. The

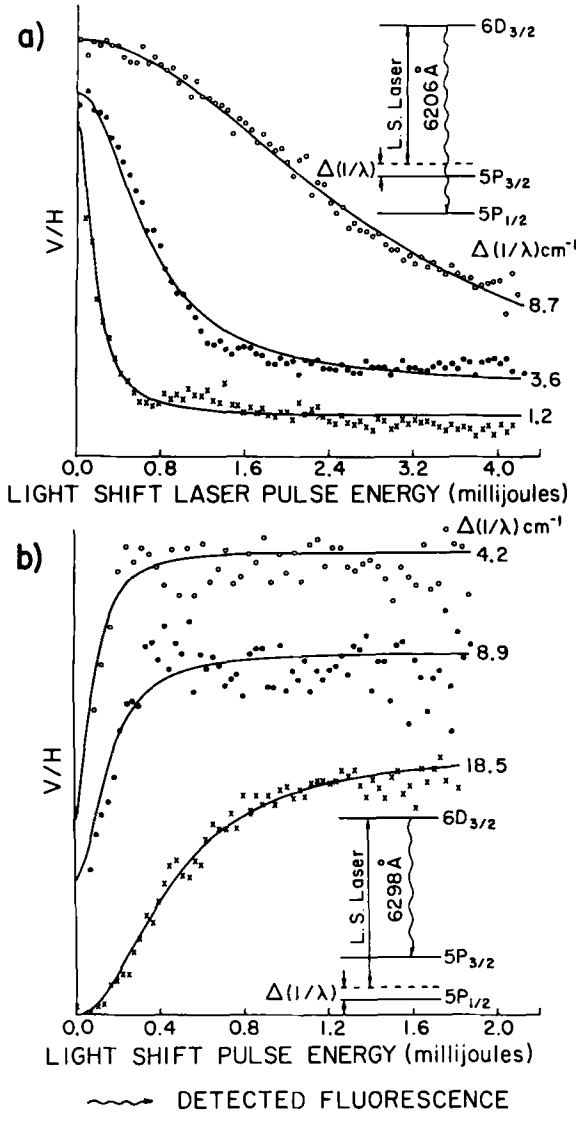

Fig. 6. Some sample data runs. Figure 6a shows data taken when the light shift laser was detuned by a small amount from the $6D_{3/2} \rightarrow 5P_{3/2}$ transition. The photomultiplier detected fluorescence resulting from $6D_{3/2} \rightarrow 5P_{1/2}$ transitions. In fig. 6b, the laser was detuned from the $6D_{3/2} \rightarrow 5P_{1/2}$ transition while fluorescence resulting from the $6D_{3/2} \rightarrow 5P_{3/2}$ transition was detected. The signal curves of figs. 6a and b are inverted with respect to each other since the signs of $B(J_a, J_f)$, listed in table 2, are opposite.

curves in fig. 6 are inverted with respect to each other since the signs of B listed in table 2 for the cases when fluorescence resulting from a $nD_{3/2} \rightarrow 5P_{1/2}$ or a $nD_{3/2} \rightarrow 5P_{3/2}$ transition is detected are opposite.

Table 3
Measured oscillator strengths

b	a	f_{ba} (expt.)	f_{ba} (theory) [22]	f_{ba} (Goltz et al.) [26]
$5P_{1/2}$	$6D_{3/2}$	0.027(5)	0.036	0.030
$5P_{3/2}$	$6D_{3/2}$	0.026(5)	0.040	0.0032
$5P_{1/2}$	$7D_{3/2}$	0.021(4)	0.024	0.020
$5P_{3/2}$	$7D_{3/2}$	0.0018(4)	0.0026	0.0020

Substituting the fluence halfwidth $F_{1/2}$ in (3.37), $|\Delta F|$ was found. (For the $J_a = 3/2$ case $F_{1/2} = |\Delta F|$.) The sign of ΔF is inferred from the theoretical formula (3.19). Finally using the two oscillator strengths $f_{5P_{1/2} \to nD_{3/2}}$ and $f_{5P_{3/2} \to nD_{3/2}}$ as free parameters, the theoretical curve (3.19) was fit to the data as shown in fig. 4. The resulting oscillator strengths are listed in table 3.

The conservative error estimate of 20% in our quoted oscillator strengths arises chiefly from the uncertainty in the fluence halfwidths. We believe the major error source is the uncertain amount of amplified spontaneously emitted (ASE) light in the laser beam. This broadband background extends over the region of the laser dye gain curve on both sides of the laser wavelength. It is therefore detuned on either side of the wavelength of the transition we wish to study. Hence, from (2.5) we seen that the ASE will not produce a net light shift. The energy meter measures the total amount of energy at all wavelengths including the amount of ASE light in the laser beam. To estimate the fraction of ASE in the laser beam, we used a high resolution (< 1 Å) monochromator to determine the laser spectral profile. We were careful to use calibrated neutral density filters to prevent photomultiplier saturation near the lasing wavelength. The ASE energy fraction of our laser pulses was estimated to be about $< 10\%$. Due to the uncertainty of this ASE estimate, we did not subtract the estimated ASE energy from the measured energy.

The energy meter measured only the fraction of the laser pulse reflected from a glass slide. The glass slide reflectivity was measured to an accuracy of 5%. The pyroelectric energy meter has an advertised accuracy of 2%. This claim was tested by measuring the average laser pulse energy using a pyroelectric and a bolometric detector. The two detector measurements agreed to within a few percent. Other possible errors such as the expansion of the laser as it travelled through the cell were determined to be small.

Our results agree quite well with measurements made by von der Goltz et al. [26]. They determined relative oscillator strengths to 10% accuracy by measuring the attenuation of probe light after it had passed through a rubidium vapor. Absolute oscillator strengths were then obtained using theoretically calculated branching ratios and measured lifetime data. Both sets of experimental measure-

ments are about 30% lower than the values obtained using the relatively simple Bates-Damgaard theory [22].

5. Conclusions

We have chosen to call this new method to measure oscillator strengths the "inverse hook method" because of its close connection to the conventional hook method [11] which is also used to measure oscillator strengths. The essence of the relationship is indicated in fig. 7. In the conventional hook method atoms of a known number density N in some energy level and of a known column length ℓ are traversed by one of two coherent optical beams which have been formed with a beamsplitter. The other optical beam passes through a reference path which

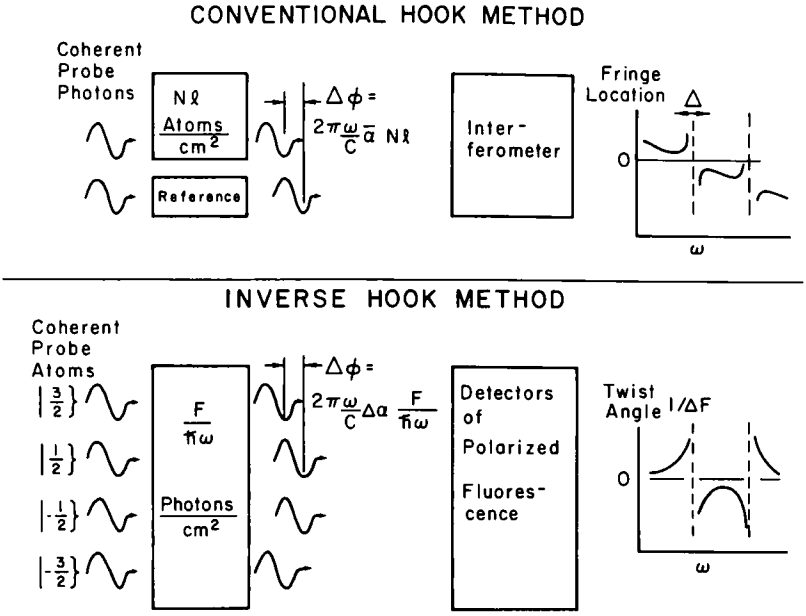

Fig. 7. Comparison of the conventional hook method and the inverse hook method. Both the conventional hook method and the inverse hook method are based on the interaction of off-resonant light with atoms. The interaction cause phase shifts between the two light beams of a conventional hook experiment, and these phase shifts are detected by an optical interferometer. In the inverse hook method the interaction cause phase shifts in the amplitudes of the $2J+1$ sublevels $|m\}$ of the atom, and these phase shifts cause the atomic polarization to twist around the direction of linear polarization of the light shift laser. The twist angle per unit fluence $1/\Delta F$ can be determined from the depolarization of the fluorescent light.

introduces a large phase retardation. The optical phase retardation $\Delta\phi$ produced by the atoms is given by

$$\Delta\phi = 2\pi\frac{\omega}{c}\bar{\alpha}N\ell \tag{5.1}$$

where ω is the optical frequency and $\bar{\alpha}$ is the mean atomic polarizability i.e.

$$\bar{\alpha} = \frac{1}{[J_a]}\sum_m \alpha(m).$$

Here we have assumed the atoms are well approximated by an optically dilute gas. After passage through the atomic vapor or the reference cell, the two beams are recombined to form interference fringes. These are dispersed in optical wavelength λ with a spectrometer to form a pattern similar to that shown in fig. 7. The large fringe displacement near atomic resonance lines due to the greatly increased polarizability together with the sloping background due to the large phase retardation of the reference path, produces "hooks" in the fringes as shown in fig. 7. It is possible to infer the phase shift $\Delta\phi$ from the hook spacing Δ, which equals $\lambda_> - \lambda_\lambda$ where $\lambda_>$ and $\lambda_<$ are the wavelengths on either side of the resonance wavelength where the interference fringes have horizontal slope. If the atomic column density $N\ell$ is known, one can use (5.1) to determine the oscillator strength. By appropriately choosing the amount of retardation introduced in the reference path, the hook spacing can be much larger than characteristic linewidths associated with collision or Doppler broadening. Therefore both the hook method and inverse hook method, which uses a light shift laser detuned from the transition of interest, are relatively insensitive to the transition lineshape. The need to have fairly large and accurately known values of $N\ell$, or more precisely

$$\left(\frac{N_a}{[J_a]} - \frac{N_b}{[J_b]}\right)\ell,$$

as was discussed in sect. 1, is one of the most serious limitations of the conventional hook method when it is used to obtain oscillator strengths for transitions between excited energy levels of atoms.

For the inverse hook method one basically interchanges the role of the atoms and photons, as indicated in fig. 7. Instead of preparing two coherent beams of light by means of an optical beamsplitter, one prepares $2J_a + 1$ coherent "beams" of excited atoms by exciting with light linearly polarized along a direction $\hat{z}$ which is tilted by an angle β from the linear polarization axis of the light shift laser. Each atomic "beam" is in one of the eigenstates $|m\}$ of $J_{\hat{z}}$ (c.f. (3.9)).

These atomic beams pass through a column density $F/\hbar\omega$ of photons from the light shift laser and each "beam" experiences a phase shift

$$\phi(m) = 2\pi \frac{\omega}{c} \alpha(m) \left(\frac{F}{\hbar\omega} \right) \tag{5.2}$$

where $\alpha(m)$ is the polarizability of atoms in the sublevel $|m\}$. Equations (5.1) and (5.2) are completely analogous except that in (5.1) a column density of atoms $N\ell$ determines a photon phase shift and in (5.2) a column density of photons $E/h\omega$ determines an atomic phase shift. Unlike the atomic column density, the laser photon column density or the pulse fluence required in inverse hook experiments, is easily measured using a pyroelectric or bolometric detector to an accuracy of a few percent. The differential atomic phase shifts cause a change in the polarization and angular distribution of fluorescent light from the excited atom. For a linearly polarized light shift laser, this is equivalent to the results of a torsion operation on the spin polarization of the excited atoms.

In conclusion, we shall give a summary of some of the advantage of the inverse hook method over existing methods for measuring oscillator strengths. A primary advantage is that atomic number densities need not be known. Hence, the inverse hook method is particularly well suited for measuring oscillator strengths for transitions between excited states. Even the study of transitions from a bound populated state to an autoionizing state [27] should be feasible since one does not need to observe fluorescence from the second level b.

A second advantage of the new method is its use of pulsed dye lasers. The high fluence of these pulses allows the determination of small oscillator strengths, which otherwise are difficult to measure. Also since dye lasers operate throughout the visible, near UV and near IR regions of the spectrum, a very large number of transitions can be studied.

An important advantage of the inverse hook method when compared to the Autler-Townes effect which also exploits the a.c. Stark interaction, is it does not require a spatially uniform beam or very precise knowledge of the temporal profile of the laser pulses. In fact, a completely chaotic distribution of coherent light sources giving rise to a laser speckle pattern, is an excellent practical choice. Unlike the Autler-Townes method, the laser is detuned from the transition of interest. Since the detuning can be chosen to be much larger than the Doppler width and the laser linewidth, the inverse hook method is relatively insensitive to both the transition lineshape and the laser spectral profile.

Finally, we would like to emphasize the new method's experimental simplicity. The three measurements it requires, namely the detuning, the laser pulse fluence and the integrated fluorescence decay signals, are all easily obtained. The method is less complex than the measurement of atomic lifetimes or quantum beats, since very short time resolution is not required. Hence, relatively inexpensive gated

integrators rather than costly transient digitizers may be used. Its application is especially easy for anyone who uses a dye laser to excite an atomic state and then measures the state's radiative lifetime. Just by splitting the pump laser beam and pumping two dye lasers, absolute transition probabilities for each possible branch, rather than a total decay rate, can be determined.

Acknowledgements

This work was part of the PhD thesis of William A. van Wijngaarden. It was supported by Lawrence Livermore National Laboratory subcontract 3181505. We are grateful to R. Solarz and J. Paisner for initial and continued encouragement. One of us (W.A. v. W.) would like to thank the Canadian National Research Council for their financial support.

References

[1] This article is an abridged version of an article to be published in Phys. Rev. A.
[2] H. Nussbaumer, J. de Physique 40 (Feb. 1979) C1 102–105.
[3] R. Stern and J. Paisner, Atomic vapor laser isotope separation, Invited paper at the First International Laser Science Conference in Dallas Texas Nov. 19, 1985.
[4] R.W. Solarz, A physics overview of AVLIS, Lawrence Livermore Laboratory Publication UCID-20343, Feb. 1985.
[5] J.I. Davis and J.A Paisner, Science technology and the industrialization of laser-driven processes, Lawrence Livermore Laboratory Publication, May 1985.
[6] E. Condon and G. Shortley, *The Theory of Atomic Spectra* (Cambridge University Press, 1953) p. 108.
[7] E. Foster, Reports on Progress in Physics 27 (1964) pp. 470–545.
[8] A. Corney, *Atomic and Laser Spectroscopy* (Clarendon Press, Oxford 1977) p. 107.
[9] Some of the various notations for the oscillator strength for a transition from a state a to a state b are related as follows. $(f_{ab})_{\text{Corney}} = (f_{ab})_{\text{Foster}} = (f(b, a))_{\text{Condon\&Shortley}}$.
[10] M. Huber and R. Sandeman, Physica Scripta, 22 (1980) 373–385.
[11] M. Huber, *Modern Optical Methods in Gas Dynamic Research*, ed. D. Dosanjh (Plenum Press, New York, 1971) pp. 85–112.
[12] G.C. Bjorklund et al., Appl. Phys. Lett. 29 (1976) 729.
[13] S. Autler and C. Townes, Phys. Rev. 100 (1955) 703–722.
[14] R. Loudon, *The Quantum Theory of Light*, 2nd edition (Oxford University Press, New York, 1983) pp. 305–307.
[15] P.P. Sorokin, J.J. Wynne and J.R. Lankhard, Appl. Phys. Lett. 22 (1973) 342.
[16] W.A. van Wijngaarden et al. Phys. Rev. Lett. 56, No. 19 (May 12, 1986).
[17] M. Françon, *Laser Speckle and Applications in Optics* (Academic Press, New York, 1979).
[18] J.C. Dainty, *Laser Speckle and Related Phenomena* (Springer-Verlag, New York, 1975).
[19] J.W. Goodman, *Statistical Optics* (John Wiley and Sons, New Yor, 1985) pp. 347–351.
[20] M.E. Rose, *Elementary Theory of Angular Momenta* (John Wiley and Sons, New York, 1957).
[21] R. Gupta et al. Phys. Rev. A 6 No. 2 (August 1972) 529–544.

[22] D.R. Bates and A. Damgaard, Phil. Trans. Roy. Soc. London 242 (1949) 101.
[23] T. Killian, Phys. Rev. 27 (1926) 578, log kT[Rb] $= 10.55 - 4132/T$ where T is in Kelvins and k = Boltzmann's constant.
[24] W.A. van Wijngaarden et al. Phys. Rev. A 33 No. 1 (Jan. 1986).
[25] E. Miron et al. IEEE Journal of Quantum Electronics, QE-15, No. 3 (March 1979) 194–196.
[26] D. von der Goltz et al., Physica Scripta 30 (1985) 244–245.
[27] U. Fano, Phys. Rev. 124 No. 6 (Dec. 1961) 1866–1878.

Discussion

G. Ravindra Kumar: In the ΔF vs frequency curve you have data at two extremes and none at the middle. How did you get such a nice fit to your data?

W. Happer: The data is fit to a curve which depends on two free parameters, the oscillator strengths for transitions from the $D_{3/2}$ state to the $^2P_{1/2}$ and $^2P_{3/2}$ states, respectively. The data is sufficient to determine these very well. No data was taken in between the two extremes because of the difficulty in suppressing instrumental scattering if the light shift laser frequency is too close to the frequency of observed fluorescence.

S.P. Tewari: I have not understood the idea of speckling. How does it help you in the experiments?

W. Happer: The speckle pattern gives one a way to obtain a predictable signal from a spatially inhomogeneous laser beam. Most pulsed dye lasers have a rather nonuniform spatial distribution which is not even reproducible from shot to shot. By speckling the beam one obtains a beam which is macroscopically uniform.

T. Nagarajan: The curves you showed do not look like a single Lorentzian. There is a distribution of Lorentzians which you can deconvolute and obtain the distribution of oscillator strengths. The distribution of oscillator strengths will come out to be Gaussian rather than exponential.

W. Happer: I believe the discrepancies you refer to are mostly random noise.